Chapter VI

Adsorption Studies using TGH

The data obtained for the removal of identified metal ions employing the third treated sorbents, TGH are discussed here.

6.1 TGH - Characterization

Microscopic view of TGH with 0.18 mm particle size is depicted in figure 6.1. Various physico-chemical parameters viz., pH, conductivity, moisture, bulk density, specific gravity, porosity, ash content, water/ acid soluble matter, ion exchange capacity, pH_{zpc}, surface acidic groups determined for TGH in the laboratory, following specific analytical techniques. All the parameters were found to possess value ranges similar to that of TPJB and TTIH, supportive of the specific sorption nature of TGH. The other parameters (surface area and mean pore diameter) were derived from BET/ BJH plots, the results being arrived from subjecting the TGH sample to BET analysis[165]. Appreciable surface area and mean pore diameter values, declare TGH to possess better metal chelating ability. The percentage of major elements (C, H, N, S) were determined using CHNS analyzer, where higher carbon content furnishes more number of active sites. The numerical data for the characteristic studies are listed in table 6.1, with corresponding BET/ BJH plots and sorption profiles (Type IV)[166], depicted in figures 6.2, 6.3 and 6.4.

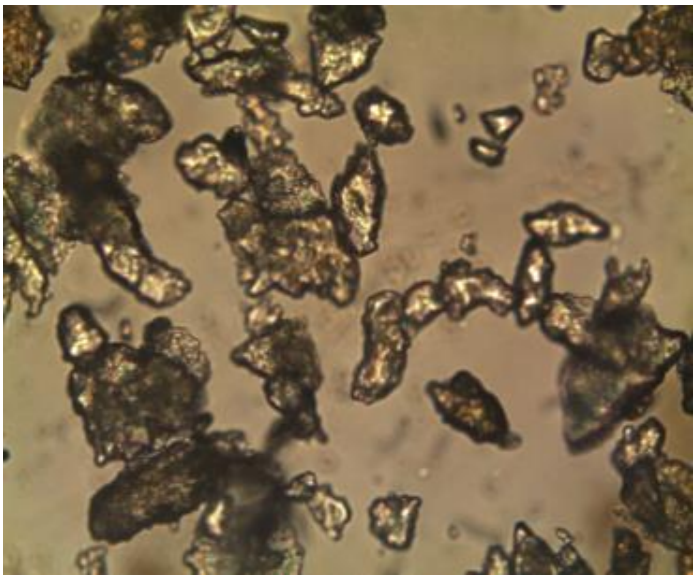

Figure 6.1 Microscopic View

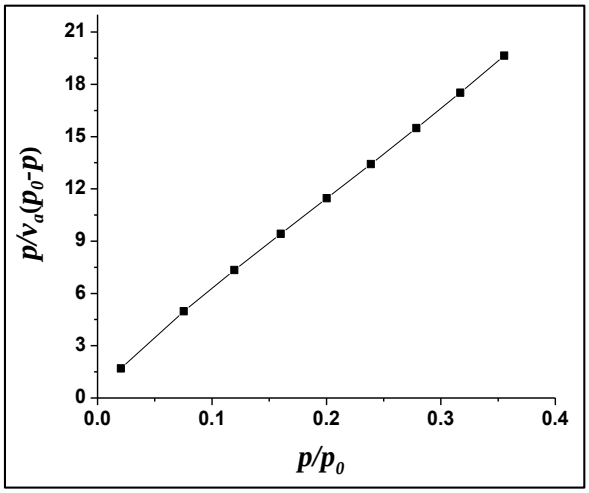

Figure 6.2 BET Plot

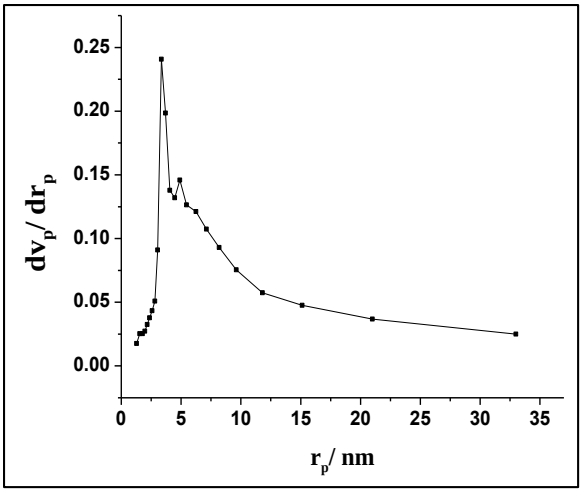

Figure 6.3 BJH Plot

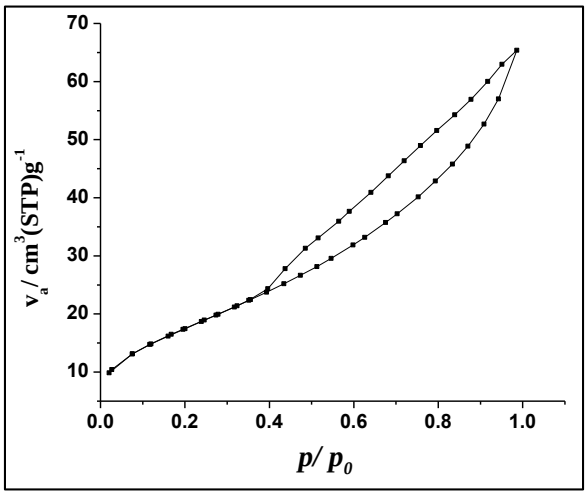

Figure 6.4 Adsorption/ Desorption Plot

Table 6.1 Physicochemical Characterization

Properties	TGH
pH (1 % solution)	7.57
Conductivity	42.65
Moisture (%)	3.18
Bulk density (g/L)	0.62
Specific gravity	1.61
Porosity	53.31
Ash content (%)	2.24
Water soluble matter (%)	1.89
Acid soluble matter (%)	1.52
Ion exchange capacity (meq/g)	0.56
pH_{zpc}	5.30
Surface area (m^2/g)	3.633
Mean Pore diameter (nm)	64.93
Carbon (%)	43.69
Nitrogen (%)	2.17
Hydrogen (%)	5.50
Sulphur (%)	2.42
Surface Acidic Groups (mmol/g)	
Phenolic	0.98
Carboxylic	2.24
Lactonic	0.12

6.2 SEM and EDAX Analyses

The SEM images of raw, treated, metal laden TGH are picturized in figures 6.5 - 6.9 Treated image shows opening up of pores on the sample surface implying a ruggedness against its raw precursor. Sorbate loaded surfaces of respective metal species indicate the occurrence of sorption at crevices, reflecting a smooth morphology. New peaks at 2 – 8 keV range for the spent TGH is evident in the EDAX spectra (Figures 6.11 – 6.13), when compared to that of treated one (Figure 6.10). This establishes the adherence of sorbate molecules onto TGH surface.

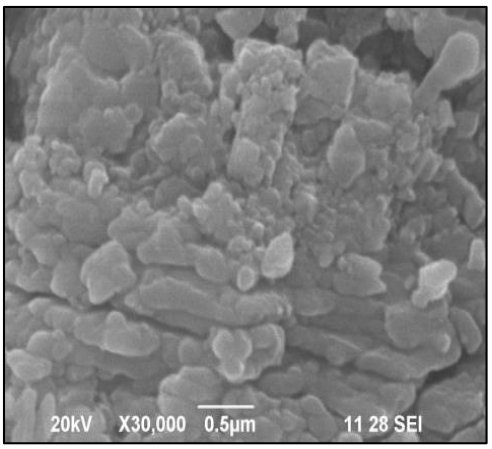

Figure 6.5 SEM: GH

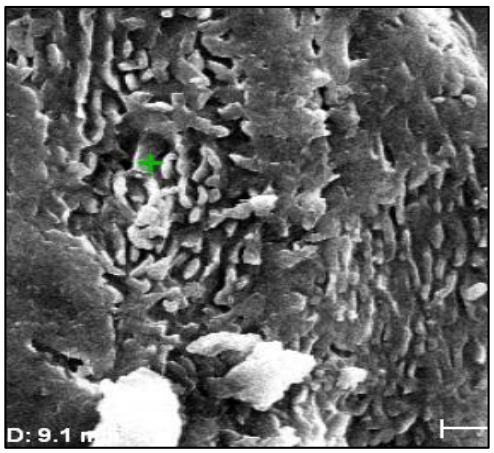

Figure 6.6 SEM: TGH

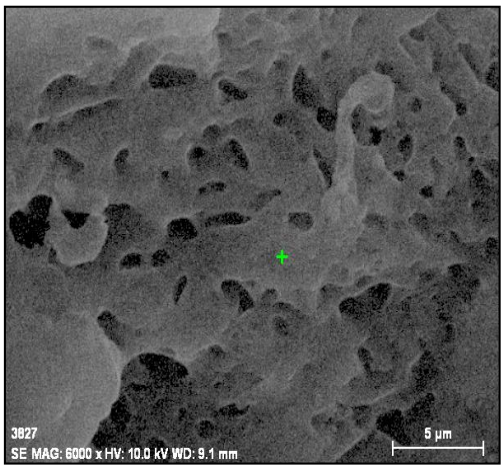

Figure 6.7 SEM: Pb(II) - TGH

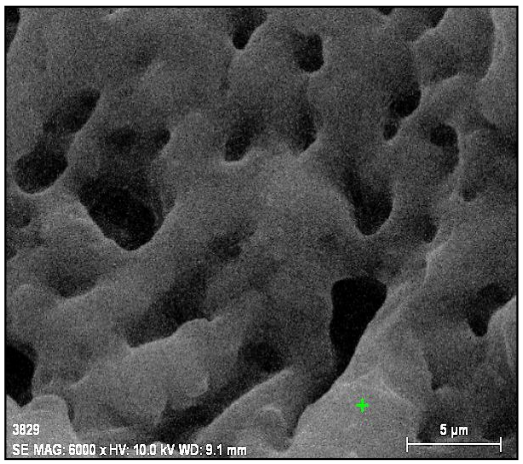

Figure 6.8 SEM: Cd(II) – TGH

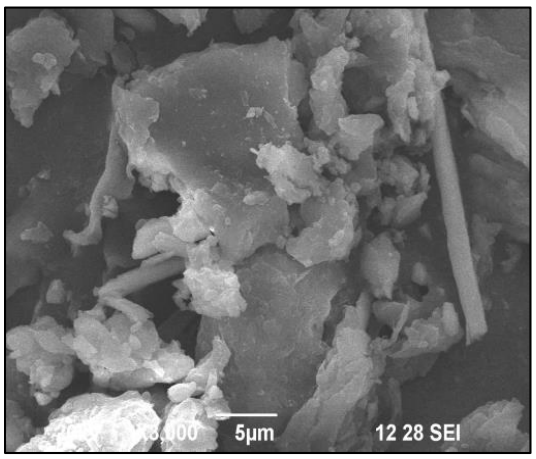

Figure 6.9 SEM: Ni(II) - TGH

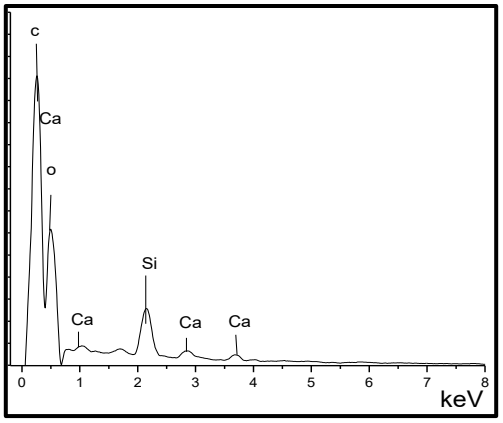

Figure 6.10 EDAX: TGH

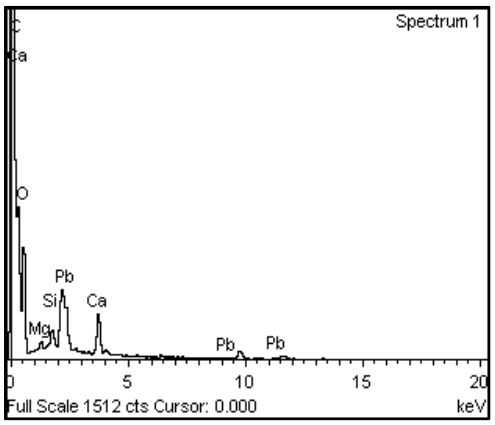

Figure 6.11 EDAX: Pb(II) - TGH

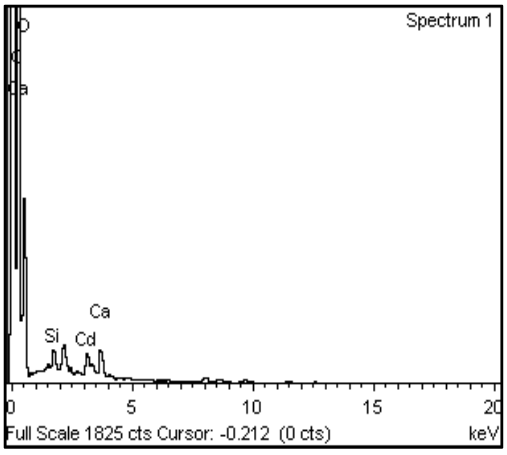

Figure 6.12 EDAX: Cd(II) - TGH

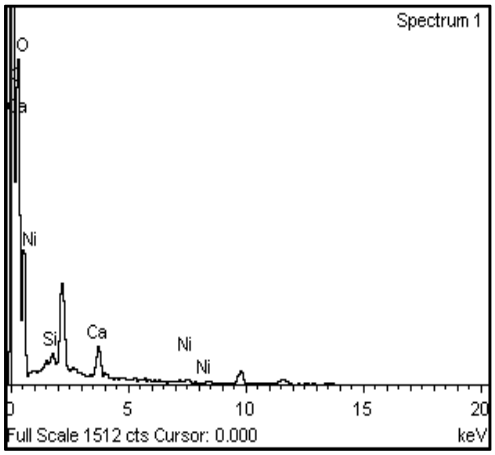

Figure 6.13 EDAX: Ni(II) - TGH

6.3 FTIR Spectral Studies

FTIR spectra recorded for systems using TGH (similar to previous results and discussions chapters) are illustrated in figure 6.14. Peak shifts/ variations in peak height, appearance/ disappearance of peaks corresponding to the transmittance/ absorbance values are disclosed in (b), (c) & (d) against their counterpart (a).

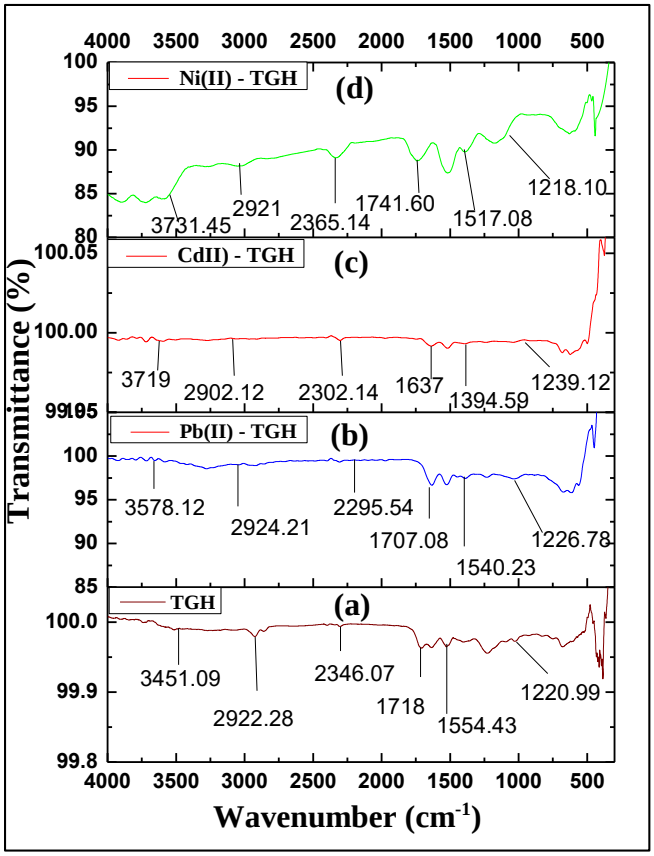

Figure 6.14 FTIR Spectra

6.4 Batch Equilibration Experiments

6.4.1 Effect of Particle Size

Table 6.2 registered the occurrence of maximum sorption for the smaller particle size[155] of 0.18 mm. The order being, Pb(II) > Cd(II) > Ni(II), alike to former discussions.

Table 6.2 Effect of Particle Size

Metal Ions	Amount Adsorbed (mg/g)				
	0.18 mm	**0.24 mm**	**0.30 mm**	**0.42 mm**	**0.71 mm**
Pb(II)	**56.76**	54.40	49.11	46.86	43.94
Cd(II)	**22.07**	21.62	19.69	18.37	16.96
Ni(II)	**20.68**	19.48	17.66	16.26	15.60

6.4.2 Effect of Initial Concentration and Agitation Time

The amounts of divalent ions adsorbed at varying initial concentrations ranging from 100 - 300 mg/L: 50 mg/L at present time course profiles (5 – 30 min: 5 min) are shown in table 6.3. The data implies a steady rise in the sorption characteristics of TGH upto 250 mg/L for Pb(II) ion, 100mg/L for Cd(II) and Ni(II) ions. This maximum sorption capacity of TGH is exhibited at 5, 10 and 20 minutes for the studied systems.

Table 6.3 Effect of Initial Concentration and Agitation Time

Metal Ions	Time (min)	Amount Adsorbed (mg/g)					
		50 mg/L	100 mg/L	150 mg/L	200 mg/L	250 mg/L	300 mg/L
Pb(II)	5	10.46	22.61	32.73	42.50	**56.89**	52.28
	10	13.63	22.26	32.43	41.51	56.01	51.56
	15	13.28	22.29	31.73	40.47	56.08	49.18
	20	12.92	22.02	31.17	39.37	55.39	47.67
	25	12.66	21.77	29.16	38.58	54.77	46.52
	30	12.30	21.27	28.34	37.48	53.52	47.24
Cd(II)	5	12.97	21.57	18.80	20.87	21.26	20.90
	10	13.14	**22.22**	19.01	21.78	21.46	20.56
	15	13.28	21.89	18.11	21.24	20.75	19.19
	20	12.76	21.10	17.76	20.17	20.63	18.36
	25	12.34	20.31	17.44	19.64	20.47	17.73
	30	12.14	20.04	17.16	18.89	20.07	16.93
Ni(II)	5	11.36	19.64	17.41	19.23	18.04	18.29
	10	12.65	20.01	17.85	19.21	18.49	17.94
	15	12.96	20.56	18.344	19.02	19.14	17.83
	20	13.41	**20.93**	18.69	19.58	19.41	18.49
	25	12.83	20.38	17.67	19.53	18.55	18.63
	30	12.63	20.19	17.16	18.89	18.28	18.29

6.4.3 Effect of Dosage

Figure 6.15 depicts the curve profiles for amounts of the divalent ions adsorbed, where sorption has occurred at 100 mg, further sloping down of curves may be due to agglomeration of particles at higher doses[159].

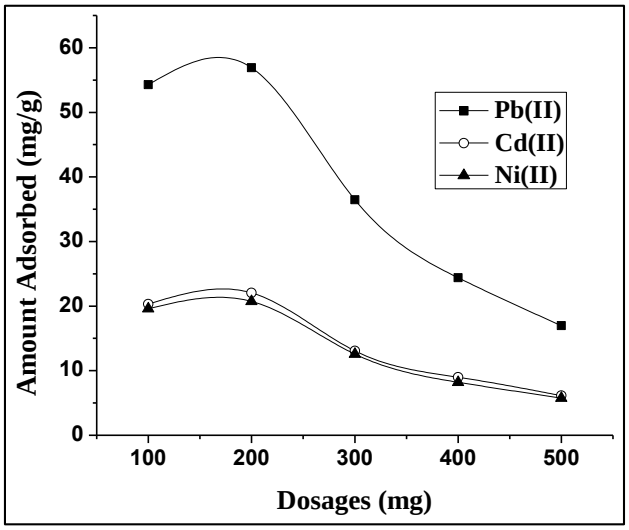

Figure 6.15 Effect of Adsorbent Dose

6.4.4 Effect of pH

pH 5 and pH 7 had found to register maximum, as evident from the inverted parabola, (Figure 6.16) of Pb(II), Ni(II) and Cd(II) ions. Preferential protonation and hydroxide precipitation may be factors, diminishing the sorption rate.

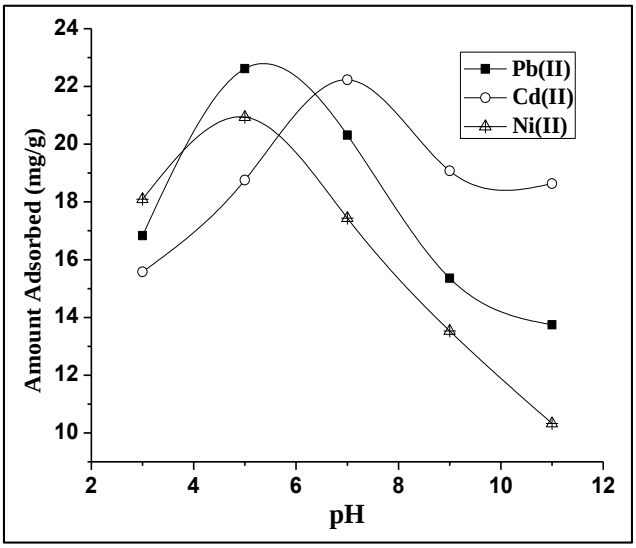

Figure 6.16 Effect of pH

6.4.5 Effect of Cations/ Anions/ Co-ions

Role of the interfering ions for bivalent ions, TGH systems as shown in table 6.4, record least inhibition of cation, anion and co-ions favoring the efficacy of TGH in trapping metal ions under ions intrusing environments.

Table 6.4 Effect of Cations, Anions and Co-ions

Metal Ions	Percentage Removal (%)						
	Absence of Ions	Cations		Anions		Co-ions	
		Mg^{2+}	K^{+}	Cl^{-}	SO_4^{2-}	Zn^{2+}	Cr^{6+}
Pb(II)	91.40	90.15	89.23	88.01	86.45	89.34	88.10
Cd(II)	89.84	88.04	87.54	86.45	84.34	87.65	86.43
Ni(II)	84.61	82.16	81.67	80.76	79.76	82.34	82.56

6.4.6 Effect of Temperature

The effect of temperature (293-333 K: 10 K intervals) on the removal of Pb(II), Cd(II) and Ni(II) are illustrated in table 6.5, where the maximum percentage is obvious at room temperature, beyond which, sorbate particles – annihilation could prevent their enhanced rate of adsorption, thereby exhibiting exothermic nature of the systems[167].

Table 6.5 Effect of Temperature

TGH	Percentage Removal (%)				
	293K	303 K	313 K	323 K	333 K
Pb(II)	82.21	91.40	88.60	88.44	89.45
Cd(II)	67.20	89.84	87.87	85.92	86.50
Ni(II)	62.33	84.61	78.31	78.97	79.13

6.4.7 Desorption and Regeneration Studies

Desorbing capacities and regenerating abilities of metal loaded TGH employing 0.01M HCl as eluent is expressed as bar diagrams in figure 6.17, where an appreciable desorption is shown as lying between 55 - 65% for the three ions at the end of 5^{th} cycle.

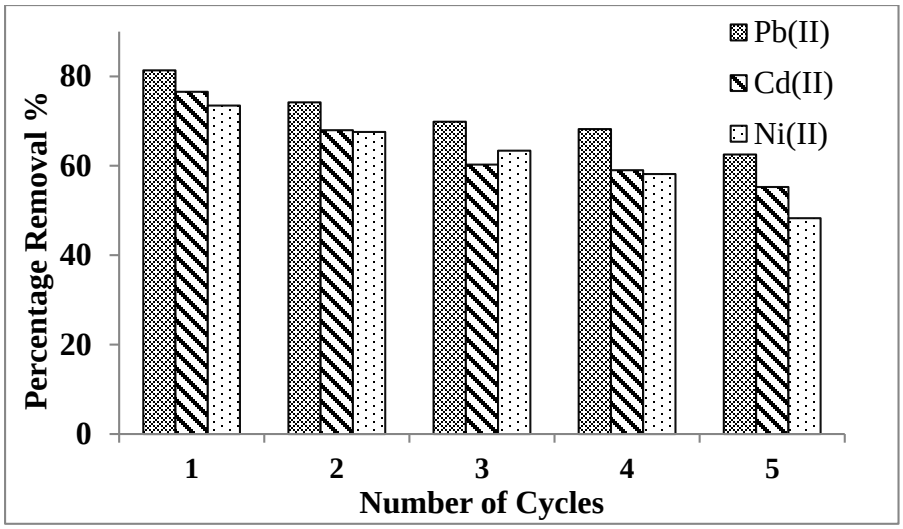

Figure 6.17 Regeneration - TGH

6.5 Adsorption Isotherms

Langmuir, Freundlich, Tempkin and Dubinin-Kaganer-Radushkevich isothermal equations applied to the batch experimental data (Table 6.6) to verify the best linear fit for the TGH systems and the calculated isothermal parameters from their respective plots are summarized in table 6.7.

Table 6.6 Equilibrium Concentrations

Conc. of Metal Ions (mg/L)	Langmuir		Freundlich		Tempkin		DKR	
	C_e	C_e/q_e	log C_e	log q_e	ln C_e	q_e	ε^2 X10^{-5}	ln q_e
Pb(II)								
50	7.10	0.67	0.85	1.01	1.96	10.46	1.10	2.34
100	8.51	0.37	0.93	1.35	2.14	22.61	0.78	3.11
150	18.02	0.55	1.25	1.51	2.89	32.73	0.18	3.48
200	28.83	0.67	1.45	1.62	3.36	42.50	0.07	3.74
250	21.41	0.37	1.33	1.75	3.06	56.89	0.13	4.04
300	78.52	1.50	1.89	1.71	4.36	52.28	0.01	3.95

Conc. of Metal Ions (mg/L)	Langmuir		Freundlich		Tempkin		DKR	
	C_e	C_e/q_e	log C_e	log q_e	ln C_e	q_e	ε^2 X10^{-5}	ln q_e
Cd(II)								
50	9.54	0.72	0.97	1.11	2.25	13.14	0.62	2.57
100	10.05	0.45	1.02	1.34	2.30	22.22	0.57	3.10
150	24.87	1.30	1.39	1.27	3.21	19.01	0.09	2.94
200	58.17	2.67	1.76	1.33	4.06	21.78	0.01	3.08
250	110.16	5.13	2.04	1.33	4.70	21.46	0.005	3.06
300	131.10	6.39	2.12	1.31	4.87	20.50	0.003	3.02
Ni(II)								
50	8.71	0.64	0.94	1.12	2.16	13.41	0.74	2.59
100	15.24	0.72	1.18	1.32	2.72	20.93	0.25	3.04
150	26.82	1.43	1.42	1.27	3.28	18.69	0.08	2.92
200	51.75	2.64	1.71	1.29	3.94	19.59	0.02	2.97
250	83.61	4.30	1.92	1.28	4.42	19.41	0.008	2.96
300	129.66	7.01	2.12	1.26	4.86	18.49	0.003	2.91

Table 6.7 Isothermal Constants

Isotherm Parameters	Pb(II)	Cd(II)	Ni(II)
Langmuir			
q_m (mg/g)	56.02	21.34	18.82
b (L/g)	0.032	0.045	0.002
R^2	0.9979	0.9954	0.9965
Freundlich			
K_F (mg/g)	15.66	9.41	7.52
n	1.68	4.71	3.68
R^2	0.9877	0.9916	0.9825

Isotherm Parameters	Pb(II)	Cd(II)	Ni(II)
Tempkin			
A_T (L/g)	16.51	11.98	5.7
b_T	2.49	1.38	1.37
R^2	0.9188	0.9578	0.9325
DKR			
q_s (mg/g)	57.77	22.39	19.61
E (kJ/mol)	3.98	8.34	7.03
R^2	0.9294	0.9443	0.9324

6.5.1. Langmuir Isotherm Model

The linear plots of C_e/ q_e vs C_e (Figure 6.18) at varying initial concentrations indicate the applicability of Langmuir model for all the three systems. Amongst the 'q_m 'values, it is observed that the amount of Pb(II) adsorbed by TGH is higher, compared to that of the other two systems. Also, the separation factor values observed from table 6.8, show the favorability of sorption process.

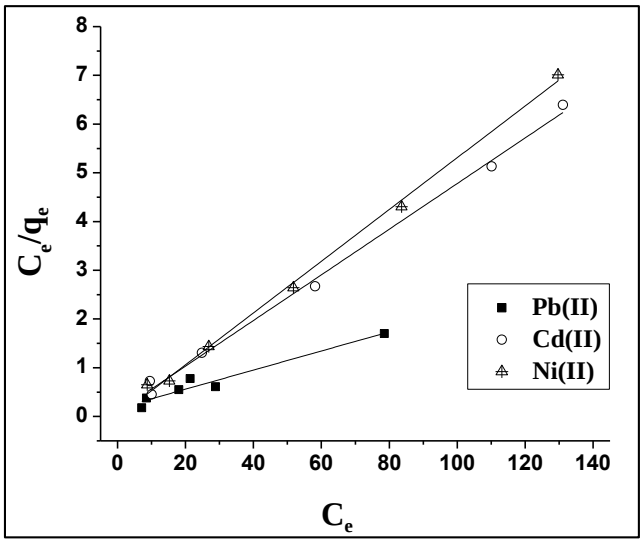

Figure 6.18 Langmuir Isotherm Model

Table 6.8 Equilibrium Parameter (R_L)

Conc. (mg/L)	Pb(II)	Cd(II)	Ni(II)
50	0.86	0.81	0.99
100	0.75	0.68	0.98
150	0.67	0.59	0.97
200	0.60	0.52	0.96
250	0.55	0.47	0.95
300	0.51	0.42	0.94

6.5.2 Freundlich Isotherm Model

Appreciable K_F and n values (Table 6.7) calculated from Freundlich plot (Figure 6.19) imply favorable nature of adsorption[140]. The linearity of plots with R^2 values nearness to unity, suggest multilayer adsorption.

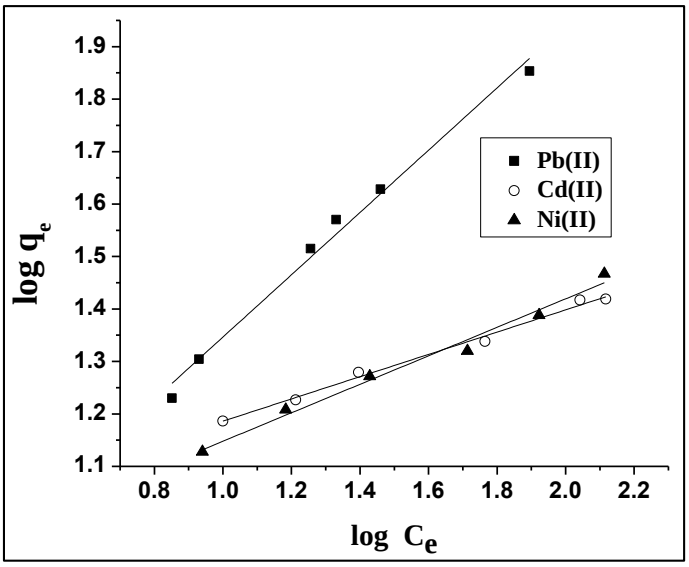

Figure 6.19 Freundlich Isotherm Model

6.5.3 Tempkin Isotherm Model

Tempkin constants A_T and b_T are related to the equilibrium binding and heat of adsorption derived from the plot of q_e vs ln C_e (Figure 6.20). The lower A_T, b_T and deviated correlation coefficient values from unity (as evident from table 6.7) corresponds to non-applicability of Tempkin model.

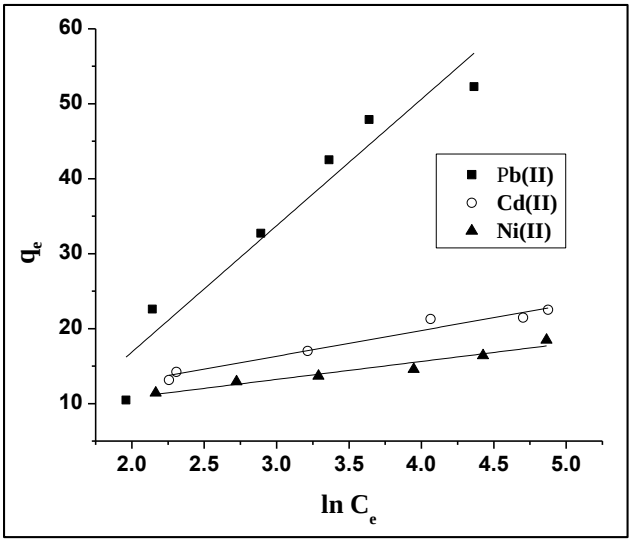

Figure 6.20 Tempkin Isotherm Model

6.5.4 Dubinin–Kaganer-Radushkevich Isotherm Model

DKR constant q_s and E were calculated from the plots ln q_e vs ε^2 (Figure 6.21). Similar to previously dealt systems, TGH also registered mean free energy values lower than 8 KJ/ mol, denoting the mechanism to be physisorption[168].

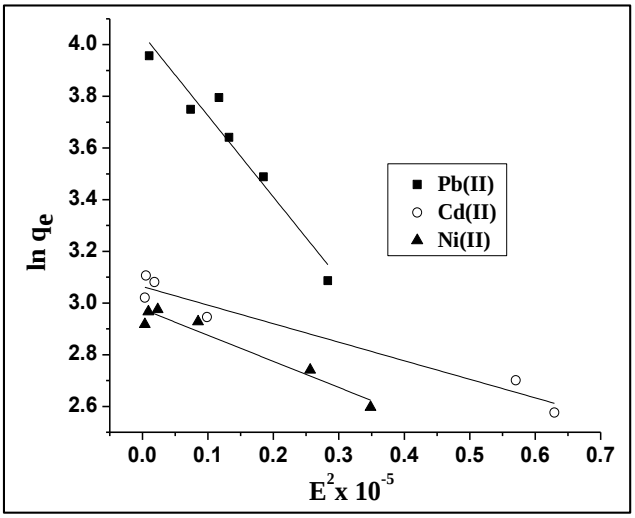

Figure 6.21 Dubinin-Kaganer-Radushkevich Isotherm Model

6.6 Adsorption Kinetics

The kinetics of Pb(II), Cd(II) and Ni(II) sorption were analyzed using pseudo-first-order, pseudo-second-order, Elovich and intraparticle diffusion models.

6.6.1 Pseudo-First-Order/ Pseudo-Second-Order Models

The data corresponding to the pseudo-first/ pseudo- second order kinetic models are represented in table 6.9 and their respective linear plots are depicted in figures 6.22 - 6.24. The sorption rate constants (K_1 and K_2), along with the corresponding q_{cal}, SSE and R^2 values determined from the slopes and intercepts of the plots are listed in table 6.10.

Better correlation coefficients and lesser SSE values observed at the optimized concentrations, in case of pseudo-second-order than pseudo-first-order kinetics suggest that the reaction follow the former model.

Table 6.9 Pseudo-First-Order / Pseudo-Second-Order Kinetics

Time (min)	Pb(II)- TGH			Cd(II)- TGH			Ni(II)- TGH		
	$\log(q_e-q_t)$	q_t	t/q_t	$\log(q_e-q_t)$	q_t	t/q_t	$\log(q_e-q_t)$	q_t	t/q_t
5	2.283	56.89	0.08	1.888	21.57	0.23	1.899	19.64	0.25
10	2.285	56.01	0.17	1.885	22.22	0.44	1.897	20.01	0.49
15	2.285	56.08	0.26	1.886	21.89	0.68	1.894	20.56	0.72
20	2.286	55.39	0.31	1.891	21.10	0.94	1.892	20.93	0.95
25	2.288	54.77	0.45	1.895	20.31	1.23	1.895	20.38	1.22
30	2.291	53.52	0.56	1.897	20.04	1.49	1.896	20.19	1.48

Table 6.10 Comparison of Pseudo-First/ Pseudo-Second-Order Kinetic Constants

Conc. of Metal Ions (mg/L)	$q_{exp.}$ (mg/g)	Pseudo-First-order Kinetics				Pseudo-Second-order Kinetics			
		$q_{cal.}$ (mg/g)	$k_1\times10^{-3}$ (min^{-1})	R^2	SSE	$q_{cal.}$ (mg/g)	$k_2\times10^{-3}$ (g/ mg min)	R^2	SSE
Pb(II)									
50	10.46	46.12	1.88	0.8724	5.94	12.55	5.95	0.9916	0.34
100	22.61	56.43	1.62	0.9093	5.63	21.14	3.85	0.9990	0.24
150	32.73	87.21	1.56	0.9062	9.08	29.57	3.24	0.9947	0.52
200	42.50	92.82	1.25	0.8924	8.38	38.67	3.25	0.9983	0.63
250	56.89	167.47	1.62	**0.8993**	**18.43**	55.19	3.34	**0.9990**	**0.28**
300	52.28	197.25	1.02	0.8509	24.16	51.55	3.23	0.9989	0.12

Conc. of Metal Ions (mg/L)	$q_{exp.}$ (mg/g)	Pseudo-First-order Kinetics				Pseudo-Second-order Kinetics			
		$q_{cal.}$ (mg/g)	$k_1 \times 10^{-3}$ (min^{-1})	R^2	SSE	$q_{cal.}$ (mg/g)	$k_2 \times 10^{-3}$ (g/ mg min)	R^2	SSE
Cd(II)									
50	13.14	34.79	1.11	0.9098	3.60	11.94	1.92	0.9972	0.20
100	22.22	42.16	1.04	**0.9123**	**3.32**	21.59	1.69	**0.9992**	**0.10**
150	19.01	53.79	0.62	0.8971	5.79	18.77	1.64	0.9972	0.04
200	21.78	69.86	0.58	0.8863	8.01	19.48	1.41	0.9954	0.38
250	21.46	82.41	0.63	0.8581	10.15	19.86	1.35	0.9958	0.26
300	20.50	94.68	0.24	0.8202	12.36	18.30	1.34	0.9993	0.36
Ni(II)									
50	13.41	35.23	1.13	0.8209	3.63	12.98	1.43	0.9961	0.07
100	20.93	59.72	0.30	**0.8552**	**6.46**	20.43	1.59	**0.9987**	**0.08**
150	18.69	74.25	0.06	0.8638	9.26	17.29	1.14	0.9945	0.23
200	19.58	81.64	0.07	0.8184	10.34	19.12	1.41	0.9983	0.07
250	19.41	95.73	0.06	0.8057	12.72	18.44	1.44	0.9968	0.16
300	18.49	134.62	0.06	0.8092	19.35	18.56	1.22	0.9989	0.01

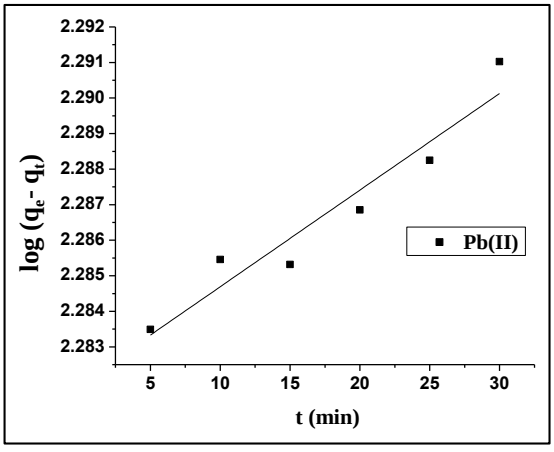

Figure 6.22 Pseudo-First-Order Kinetics – Pb(II)

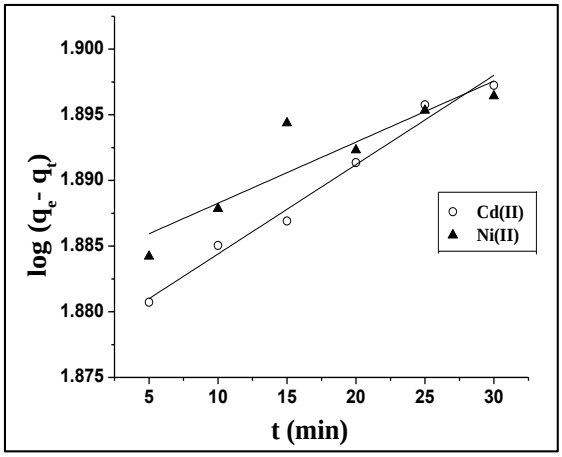

Figure 6.23 Pseudo-First-Order Kinetics – Cd(II) and Ni(II)

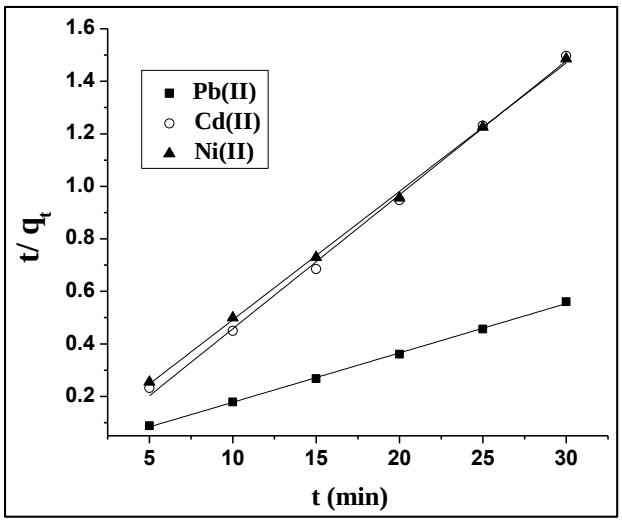

Figure 6.24 Pseudo-Second-Order Kinetics

6.6.2 Elovich Model

The Elovich co-efficients are computed from the plots q_t vs ln t (Figures 6.25, 6.26). The constants α, β was found to increase with the concentrations of divalent ions invariably for the all the systems (Table 6.11), exhibit the better sorptive nature at lower concentrations.

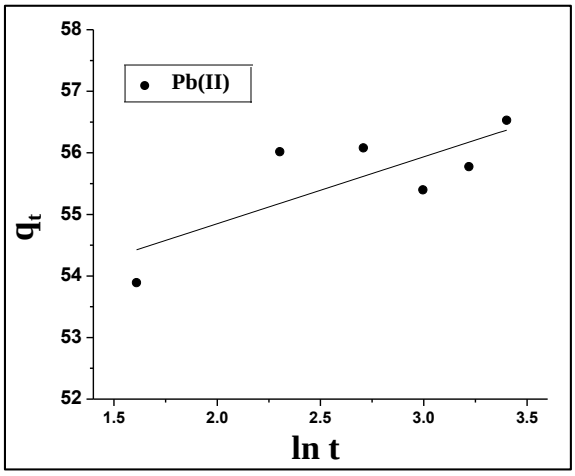

Figure 6.25 Elovich Model – Pb(II)

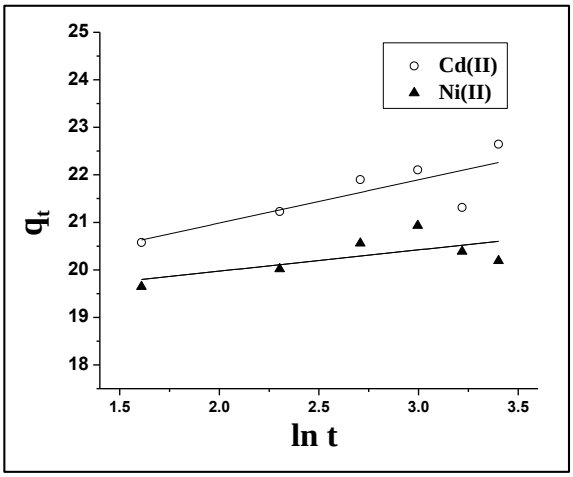

Figure 6.26 Elovich Model – Cd(II) and Ni(II)

Table 6.11 Elovich Constants

Conc. of Metal Ions (mg/L)	Pb(II)			Cd(II)			Ni(II)		
	α	β	R^2	α	β	R^2	α	β	R^2
50	0.64	10.26	0.8139	0.47	14.04	0.8309	0.08	10.53	0.8529
100	0.83	23.75	0.8709	0.96	23.79	0.8488	0.44	19.07	0.8095
150	2.37	37.36	0.8713	1.01	20.80	0.8713	0.60	17.67	0.8251
200	2.74	47.40	0.8259	1.17	23.60	0.8641	0.71	19.22	0.8925
250	2.59	59.76	0.9079	1.68	22.63	0.9126	1.29	17.85	0.8722
300	3.41	58.32	0.8356	2.26	25.05	0.9016	2.17	17.78	0.8034

α: (mg/g min), β: (g/mg)

6.6.3 Intraparticle Diffusion Model

The boundary layer diffusion, followed gradual adsorption is evident from the intraparticle diffusion plots (Figures 6.27 and 6.28). The K_i and C values (Table 6.12), is observed to be directly proportional to metal concentrations. This shows that a resistance is developed at the boundary layer, diminished its thickness, due to the transfer of sorbate mass[148].

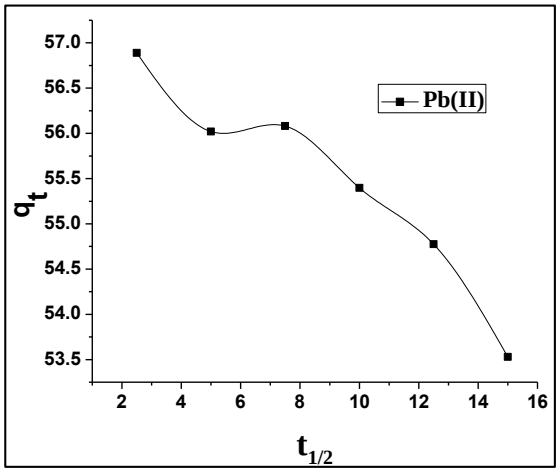

Figure 6.27 Intraparticle Diffusion Model – Pb(II)

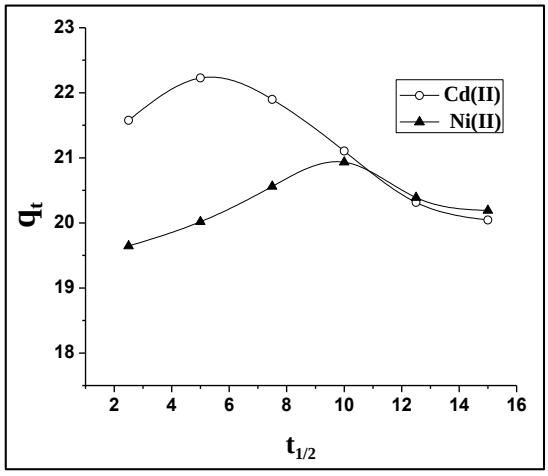

Figure 6.28 Intraparticle Diffusion Model – Cd(II) & Ni(II)

Table 6.12 Intraparticle Diffusion Constants

Conc. of Metal Ions (mg/L)	Pb(II)		Cd(II)		Ni(II)	
	K_i (mg/g $min^{1/2}$)	C	K_i (mg/g $min^{1/2}$)	C	K_i (mg/g $min^{1/2}$)	C
50	0.06	11.95	0.08	13.48	0.13	1.50
100	0.09	22.88	0.16	22.61	0.08	11.90
150	0.36	34.16	0.15	19.38	0.04	19.86
200	0.40	43.49	0.19	2.17	0.01	18.08
250	0.24	57.57	0.10	21.68	0.02	19.26
300	0.47	53.25	0.33	21.83	0.03	17.97

6.7 Adsorption Dynamics

The ΔH^0, ΔS^0 calculated from the slope and intercept of Vant Hoff plot (Figure 6.29) are shown in table 6.13. The negative values obtained for parameters ΔG^0 and ΔH^0 indicate the feasibility, spontaneous and exothermic nature of the systems. Positive values of ΔS^0 suggest increased randomness at the sorbate-sorbent interface. Similar trend had been reported for studies employing tamarind seeds[109] and sawdust[155] as sequestering agent.

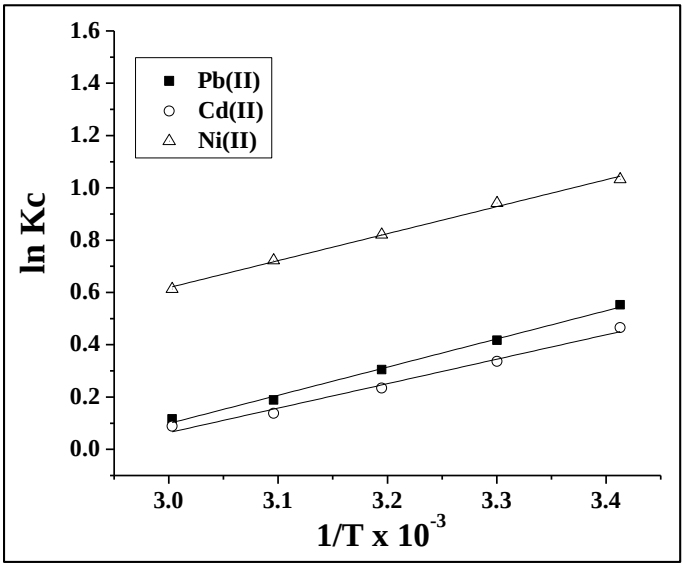

Figure 6.29 Vant Hoff's Plot

Table 6.13 Thermodynamic Constants

Temp. K	Pb(II)			Cd(II)			Ni(II)		
	$\Delta G°x10^{-3}$ kJ/mol	$\Delta H°$ kJ/mol	$\Delta S°$ J/mol K	$\Delta G°x10^{-3}$ kJ/mol	$\Delta H°$ kJ/mol	$\Delta S°$ J/mol K	$\Delta G°x10^{-3}$ kJ/mol	$\Delta H°$ kJ/mol	$\Delta S°$ J/mol K
293	-1.01			-2.99			-3.51		
303	-1.05			-0.58			-0.60		
313	-0.27	-8.95	26.05	-0.08	-7.78	22.78	-1.72	-8.57	20.59
323	-0.23			-0.36			-1.67		
333	-0.53			-0.24			-1.69		

6.8 Effect of TGH on Industrial Effluents

The influences of TGH in chelating the effluent samples (3.8) are expressed as a plot of the removal percentage of the chosen ions against varying doses of TGH (Figure 6.30). The inclined curves depict a maximum sorption had occurred at a dose of 500 mg being an optimum amount for the systems.

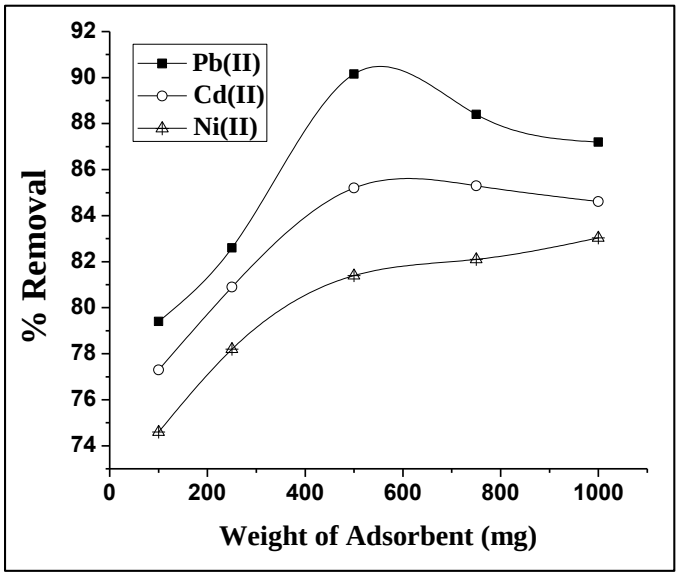

Figure 6.30 Effect of TGH on Effluent / Synthetic Solutions

6.9 SPSS Software Analysis

Batch experimental data determined for all the nine systems under their optimized conditions, are verified using SPSS 20 software. In this view point, varied parameters

viz., Descriptive, Pearson Correlation and ANOVA of the three TPJB, TTIH and TGH were statistically calculated and presented in tables 6.14(a), 6.14(b) and 6.14(c). The comparison between the descriptive parameters reveal high mean, standard deviation and standard error values for the TGH system, confirming the statement of most favoured system as discussed before. Pearson co-efficient values found to be negative for many parameters of all the systems, support appreciable adsorption.

Probability (P) values lesser than the significant value (0.05), indicate the rejection of null hypothesis for all the nine systems. F values, referring to the calculated values mean between sorbate and sorbate species is obvious to be greater than F_{cric} values. These significant differences vary with the metal removal rate.

Table 6.14(a) Statistical Analyses – TPJB

System	Parameter	Descriptive			Pearson Correlation	P	ANOVA	
		Mean	SD	SE			F	F_{crit}
Pb(II)-TPJB	Particle size	12.56	1.41	0.63	-0.9440	0.0493	33.10	5.56
	Contact time	13.55	0.50	0.20	-0.1775	0.0186	7.86	4.73
	Initial. Conc.	12.15	1.79	0.89	-0.4190	0.0129	12.21	5.24
	Dosage	12.03	2.80	1.25	-0.8517	0.0035	16.57	5.82
	pH	11.42	2.04	0.91	-0.5556	0.0304	6.88	5.96
Cd(II)-TPJB	Particle size	12.25	0.97	0.43	-0.9226	0.0416	27.98	5.27
	Contact time	13.37	0.27	0.11	-0.3541	0.0178	8.01	4.88
	Initial. Conc.	11.52	2.45	1.22	-0.6286	0.0126	12.34	5.20
	Dosage	11.16	3.07	1.37	-0.8387	0.0035	16.67	5.81
	pH	9.44	3.00	1.34	-0.5470	0.0245	7.56	5.76
Ni(II)-TPJB	Particle size	10.31	1.45	0.65	-0.8896	0.0366	22.94	5.94
	Contact time	11.89	0.41	0.17	-0.1507	0.0127	9.14	4.47
	Initial. Conc.	10.25	2.53	1.07	-0.5027	0.0120	12.62	5.63
	Dosage	10.07	2.47	1.10	-0.7868	0.0034	16.80	5.85
	pH	8.52	2.49	1.11	-0.7286	0.0420	7.72	5.44

Table 6.14(b) Statistical Analyses – TTIH

System	Parameter	Descriptive			Pearson Correlation	P	ANOVA	
		Mean	SD	SE			F	F_{crit}
Pb(II)-TTIH	Particle size	10.98	1.46	0.65	-0.6729	0.0224	58.79	5.37
	Contact time	12.89	0.68	0.27	-0.8469	0.0160	8.36	4.94
	Initial. Conc.	11.50	2.36	1.05	-0.6441	0.0044	15.33	4.64
	Dosage	10.84	2.71	1.21	-0.8037	0.0034	16.71	5.17
	pH	10.91	2.34	1.05	-0.4442	0.0571	7.92	5.28
Cd(II)-TTIH	Particle size	10.69	1.42	0.63	-0.9469	0.0227	57.24	5.67
	Contact time	11.99	0.75	0.30	-0.9613	0.0131	9.06	4.72
	Initial. Conc.	10.90	2.30	1.03	-0.6520	0.0043	15.46	4.46
	Dosage	10.07	2.73	1.22	-0.7772	0.0034	16.80	5.31
	pH	10.16	2.17	0.97	-0.2340	0.0102	6.39	5.87
Ni(II)-TTIH	Particle size	7.23	1.16	0.52	-0.9110	0.0118	48.48	5.48
	Contact time	11.70	0.60	0.24	-0.8023	0.0123	9.28	4.21
	Initial. Conc.	9.68	2.24	1.00	-0.4257	0.0041	15.73	4.73
	Dosage	9.21	1.82	0.81	0.5627	0.0033	16.90	5.92
	pH	9.37	2.11	0.94	-0.6302	0.0201	6.94	5.28

Table 6.14(c) Statistical Analyses – TGH

System	Parameter	Descriptive			Pearson Correlation	P	ANOVA	
		Mean	SD	SE			F	F_{crit}
Pb(II)-TGH	Particle size	50.21	5.29	2.36	-0.9026	0.0023	42.31	5.38
	Contact time	55.44	1.17	0.48	-0.9625	0.0014	17.20	4.96
	Initial. Conc.	36.25	17.80	7.26	0.9656	0.0051	12.73	4.98
	Dosage	37.80	17.68	7.90	-0.9575	0.0061	13.57	5.23
	pH	17.77	3.63	1.62	-0.5842	0.0010	24.99	5.41
Cd(II)-TGH	Particle size	19.74	2.15	0.96	-0.9388	0.0041	41.64	5.61
	Contact time	29.19	0.87	0.35	-0.8685	0.0358	10.92	4.69
	Initial. Conc.	19.69	3.40	1.39	-0.5855	0.0022	16.51	4.83
	Dosage	14.10	6.92	3.09	-0.9442	0.0037	16.31	5.21
	pH	18.85	2.35	1.05	-0.5842	0.0001	45.17	5.52
Ni(II)-TGH	Particle size	17.94	2.13	0.95	-0.8821	0.0082	34.54	5.74
	Contact time	20.28	0.44	0.18	0.5038	0.0483	9.53	4.16
	Initial. Conc.	18.42	2.59	1.06	-0.4474	0.0021	16.79	4.82
	Dosage	13.36	6.66	2.98	-0.9524	0.0036	16.40	5.91
	pH	16.06	4.15	1.85	-0.8728	0.0046	15.07	5.65